Impurity Sn-related paramagnetic defects in UV-illuminated $ZnWO_4$ single crystals



1999 J. Phys.: Condens. Matter 11 1333

(http://iopscience.iop.org/0953-8984/11/5/018)

J. Phys.: Condens. Matter **11** (1999) 1333–1340. Printed in the UK PII: S0953-8984(99)96918-7

# Impurity Sn-related paramagnetic defects in UV-illuminated $ZnWO_4$ single crystals

A Watterich†§, L A Kappers‡‖ and O R Gilliam‡¶

† Research Institute for Solid State Physics and Optics, Hungarian Academy of Sciences, Konkoly-Thege M út 29-33, 1121 Budapest, Hungary

‡ Department of Physics and Institute of Materials Science, University of Connecticut, Storrs, CT 06269-3046, USA

Received 21 August 1998, in final form 3 November 1998

**Abstract.** Electron spin resonance methods are used to characterize a new Sn-impurity-perturbed $W^{5+}$ centre with $C_1$ symmetry produced in $ZnWO_4$ single crystals illuminated at 77 K with 365 nm UV light. The new centre is electron-like with its highest spin density at a W site, but also with a substantial spin density at an Sn impurity substituting for a neighbouring Zn cation. It is denoted as a $W^{5+}$–$Sn^{4+}_{Zn}$ centre. The concentration of this defect is estimated to be less than 1 $\mu$mol mol$^{-1}$.

## 1. Introduction

Zinc tungstate ($ZnWO_4$) single crystals of excellent optical quality are available for practical applications as scintillation detectors [1–3] and laser hosts [4], which makes studies of point defects prior to and after various treatments and irradiations of special interest. In addition, the electron spin resonance (ESR) signals in $ZnWO_4$ are usually very narrow at low temperatures since spin–lattice interactions are small, and since the host ions have isotopes with nuclear spin only in low relative abundances such that hyperfine (HF) and superhyperfine (SHF) interactions do not cause significant line-broadening. The narrow lines make the study of defects favourable, even for those with low concentrations.

In this work we report the presence of Sn impurity in low concentration in undoped $ZnWO_4$ crystals. This impurity is detected by the appearance of a new electron-type paramagnetic defect in the crystal after UV illumination at 77 K. Characterization of the centre by ESR spectroscopy positively identifies the impurity as Sn.

The following impurity-related ions have been previously reported in $ZnWO_4$ single crystals: hydrogen in the form of $OH^-$ ions substituting for $O^{2-}$ ions [5, 6], divalent (Fe, Mn, Cu, Co and Rh [7–11]) and trivalent (Pt, Fe and Cr [11–13]) impurity cations substituting for $Zn^{2+}$ (where some of the impurities cause detrimental optical absorption in the range of the intrinsic luminescence) and the $Mo^{6+}$ impurity ion substituting for $W^{6+}$ and modifying the luminescence of the crystal [14].

Several radiation damage centres have also been identified by ESR in $ZnWO_4$. Prominent electron-like centres are the anion-vacancy-related defects and the $Me^{5+}$-type centres. Irradiation with 1.5 MeV electrons at 300 K produced the intrinsic $V^{\cdot}_O$(A) and $V^{\cdot}_O$(B) centres

§ E-mail address: watter@power.szfki.kfki.hu.
‖ E-mail address: kappers@uconnvm.uconn.edu.
¶ E-mail address: gilliam@uconnvm.uconn.edu.

0953-8984/99/051333+08$19.50  

(an electron trapped at an oxygen vacancy in the A and B positions, respectively) [15]. In Li-doped $ZnWO_4$ with a high concentration of substitutional $OH^-$ ions a $W^{5+}$-type centre in $C_1$ symmetry was found [16] after irradiation at 77 K by UV light or by $\gamma$ or x-rays. The strongest nuclear moment interaction was with W nuclei, but from ENDOR measurements another observed nuclear interaction was proved due to a nearby hydrogen which caused the symmetry reduction. This centre was denoted as $W^{5+}$–H [17]. A very similar centre ($Mo^{5+}$–H) was also observed where the strongest nuclear interaction resulted from a Mo impurity ion that substituted for the W [17].

## 2. Experimental methods and crystal structure

Single crystals of $ZnWO_4$ were grown in air by a balance-controlled Czochralski technique using Pt crucibles [18]. The raw materials were prepared from analytical grade $Na_2WO_4$ and ZnO (REANAL) by a novel method based on homogenous precipitation and liquid–liquid extraction techniques, respectively [19]. Also some crystals were grown from the best available Johnson Matthey raw materials. ESR measurements were made using a Varian X-band spectrometer equipped with an Air Products Heli-Tran accessory for low temperatures. For UV illuminations at 365 nm, a low power Hg lamp with appropriate filter was employed. To fit the experimental data the computer program 'VisualEPR' by V Grachev was used.

Zinc tungstate is a monoclinic crystal with the space group $C_{2h}^4$ ($P2/c$) [20, 21]. The two zinc and the two tungsten ions in a unit cell are magnetically equivalent having $C_2$ local symmetry. Impurity centres at Zn or W sites without any nearby lattice defects conserve the original $C_2$ symmetry and give only one ESR spectrum for an arbitrary orientation of the magnetic field $\boldsymbol{B}$. If the centre is accompanied by a nearby imperfection of the lattice, the local symmetry will be reduced to $C_1$ and then the number of spectra is increased to two according to the two geometrically different defect sites. However, for $\boldsymbol{B}$ oriented in the (010) plane or along crystallographic axes the two spectra are superposed.

## 3. Results and discussion

*As received* $ZnWO_4$ crystals show the ESR spectra of the usual impurity ions ($Fe^{3+}$, $Cr^{3+}$, $Pt^{3+}$, $Mn^{2+}$, $Rh^{2+}$ and $Cu^{2+}$); however, illumination with UV (365 nm) light at 77 K enhances the $Fe^{3+}$ intensity and two new spectra appear. Optical absorption studies have earlier shown that $Fe^{2+}$ ions are also present in $ZnWO_4$ crystals and are associated with a broad absorption band at 460 nm [7]. The illumination at 365 nm liberates electrons from $Fe^{2+}$ ions creating $Fe^{3+}$ ions; this is confirmed by an observed increase of the ESR signal due to $Fe^{3+}$. The released electrons are captured to produce two new defects. One of these will be discussed below and it will be verified that it is an electron-type defect. This new centre is still stable at 250 K, but is unstable at 300 K.

An ESR spectrum of the new centre is shown in figure 1 for $\boldsymbol{B}$ along [001]. Although two spectra are observed for an arbitrary orientation, corresponding to $C_1$ symmetry, the spectra coincide for the orientation shown in the figure. Around the most intense or central line there are four doublets with smaller intensity; two of them near the central line are somewhat larger in intensity than the other two with the larger splittings. All of these doublets are caused by nuclear interactions with isotopes of $I = 1/2$ and natural abundances much smaller than 100%. The intensity of the main line is attributed to isotopes with $I = 0$. In figure 1 the two pairs of larger lines with lesser splittings are due to $^{183}W$ nuclei (in two different W sites labelled $W_1$ and $W_2$) and the two pairs of smaller lines with greater splittings are due to $^{119}Sn$ and

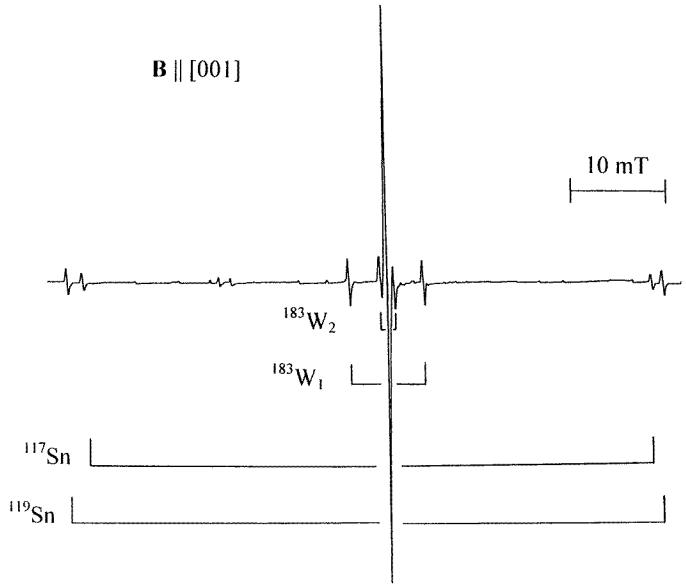


**Figure 1.** ESR spectrum of the $W^{5+}$–$Sn^{4+}_{Zn}$ centre measured at ∼23 K and ∼9.2 GHz for $\boldsymbol{B}$ along [001] in a $ZnWO_4$ single crystal after 365 nm irradiation at 77 K. The $^{119}$Sn, $^{117}$Sn and the two different $^{183}$W nuclear interactions are indicated by stick diagrams.

**Table 1.** Intensity and splitting ratios for W and Sn isotopes. Information on the isotopic natural abundances and nuclear magnetic moments was obtained from [22].

| Isotope | Abundance (%) | $I_N$ | Expected intensity ratio | Measured intensity ratio |
|---|---|---|---|---|
| $^{183}$W | 14.31 | 1/2 | $I_{main}$:$I_{W183}$ = 12.0:1 | 12:1 |
| $^{119}$Sn | 8.59 | 1/2 | $I_{W183}$:$I_{Sn119}$ = 1.67:1 | 1.7:1 |
| $^{117}$Sn | 7.68 | 1/2 | $I_{Sn119}$:$I_{Sn117}$ = 1.12:1 | 1.1:1 |
| $^{115}$Sn | 0.34 | 1/2 | $I_{Sn119}$:$I_{Sn115}$ = 25.3:1 | 27:1 |

| Isotope | $\lvert\mu_I\rvert$ | Expected splitting ratio | Measured splitting ratio |
|---|---|---|---|
| $^{119}$Sn | 1.0473 | $\lvert\mu_{Sn119}$:$\mu_{Sn117}\rvert$ = 1.046:1 | 1.038:1 |
| $^{117}$Sn | 1.0010 | $\lvert\mu_{Sn119}$:$\mu_{Sn115}\rvert$ = 1.140:1 | 1.139:1 |
| $^{115}$Sn | 0.9188 | | |

$^{117}$Sn isotopes. These assignments are labelled on the figure. At some orientations even the lines of $^{115}$Sn with small natural abundance (0.34%) could be observed. Verification of these assignments results from the excellent agreement of measured intensity ratios (of the doublet lines to the main line) with expected intensity ratios calculated from isotopic abundances. These ratios are shown in table 1. Since HF or SHF splittings are proportional to the nuclear magnetic moments, the ratios of the magnetic moments of the different Sn isotopes should be equivalent to the ratios of the splittings. This is also shown in table 1 and provides additional proof of Sn impurity.

For determination of spin-Hamiltonian parameters of the Sn-related centre, angular variations of the ESR spectra were taken in three different planes. The spin Hamiltonian employed was

$$\mathcal{H}_S = \mu_B \boldsymbol{S} \cdot \tilde{\mathbf{g}} \cdot \mathbf{B} + \sum (\boldsymbol{S} \cdot \tilde{\mathbf{A}}_i \cdot \boldsymbol{I}_i - g_N \mu_N \mathbf{B} \cdot \boldsymbol{I}_i) \qquad (1)$$

where $i$ denotes a specific interacting nucleus ($W_1$, $W_2$ or Sn), $S = 1/2$, $I_i = 1/2$, and where $\tilde{\mathbf{A}}_i$ represents either a HF or SHF tensor. The computer-fit spin-Hamiltonian parameters of the new centre are shown in table 2. Angular variations of the central ESR lines, the $^{183}W_1$ HF lines and the $^{119}$Sn SHF lines for two planes are shown in figures 2(a)–(c), respectively. Angular variations of the $^{183}W_2$ SHF lines are not shown (due to limited line resolution) and its $\tilde{\mathbf{A}}$ tensor was not determined. In the figures the squares represent experimental data and the solid curves are computer-simulated angular variations calculated with the optimized spin-Hamiltonian parameters.

Values of HF and SHF interactions with W and Sn nuclei are suitably presented in a transformed form: $\tilde{\mathbf{A}} = A_{iso}\tilde{\mathbf{1}} + \tilde{\mathbf{B}}$, where $A_{iso}$, $\tilde{\mathbf{1}}$ and $\tilde{\mathbf{B}}$ are the isotropic hyperfine coupling constant (given by $A_{iso} = -8\pi/3|\Phi(0)|^2\mu_B\mu_N$), the unit tensor and the traceless tensor of the anisotropic hyperfine coupling, respectively. The diagonalized components are: $B_{xx} = -b+b'$, $B_{yy} = -b-b'$ and $B_{zz} = 2b$, where $b$ is the axial part and $b'$ is a measure of the deviation from axial symmetry. In this form the computed HF and SHF parameters in units of $10^{-4}$ cm$^{-1}$ are the following: for the $^{183}W_1$ HF, $A_{iso} = 83.8$, $b = 21.1$ and $b' = 10.4$; for the $^{119}$Sn SHF, $A_{iso} = 451.9$, $b = 5.9$ and $b' = -2.45$. The ratio of the $A_{iso}$ values divided by the corresponding magnetic moments, namely, $(A_{iso}/\mu)_{W1}/(A_{iso}/\mu)_{Sn}$, equals 1.65. This shows that the spin density at the $W_1$ nucleus is greater than at the Sn nucleus; thus the $^{183}W_1$ nuclear interaction is denoted as HF. Since the principal $g$ values of the new centre (table 2) are less than the free electron value ($g_e = 2.0023$), the centre is electron-like. Because $S = 1/2$ and because of the strong spin density on a $W_1$, the new centre is basically a $W^{5+}$ centre, whose electron configuration is $5d^1$. Indeed, the principal values and eigenvectors of the **g** tensor and the $W_1$ HF tensor of the new centre are much closer to those of the $W^{5+}$–H centre than to those of the $V_O^{\cdot}$(B) centre (table 2), which was modelled as an electron trapped at an anion vacancy with spin density on neighbouring W nuclei.

The impurity giving strong SHF interactions in the new centre is Sn; this element is normally in the 4+ or 2+ charge state. Since $A_{iso} \gg b$ for the Sn interactions, the electron's interaction with the Sn is primarily of s character. Its wavefunction overlap contributes to the Sn's +3 charge state with electron configuration $5s^1$ rather than the +1 charge state with configuration $5p^1$. Since the spin density is larger at the $W_1$ site rather than the Sn, the defect is represented with the $W^{5+}$ notation and the Sn is considered as a perturbation in the form of $Sn^{4+}$. In further substantiation of this, the unpaired spin of the $Sn^{3+}$ ion in $Be_3Al_2Si_6O_{18}$:Sn crystals x-irradiated at 77 K [23] was reported to have a high spin density at the Sn nucleus with its $A_{iso}$ value an order of magnitude larger than the Sn $A_{iso}$ value reported here.

Furthermore, the ionic radii of $Sn^{2+}$ and $Sn^{4+}$ ions are 0.093 and 0.071 nm, respectively, while those of the $Zn^{2+}$ and $W^{6+}$ ions are 0.074 and 0.062 nm, respectively. The larger $Sn^{2+}$ ion might not be accommodated by the $ZnWO_4$ lattice; however, the smaller $Sn^{4+}$ should substitute easily for $Zn^{2+}$. Additionally, $Sn^{4+}$ at a W site is unlikely because it would be expected to have an accompanying charge-compensating oxygen vacancy which would make it resemble the $V_O^{\cdot}$(B) centre more than the $W^{5+}$–H centre; but this is not the case. Moreover, the complete disagreement of the eigenvectors of the Sn SHF tensor with those of the W in the $Mo^{5+}$–H centre is also supportive of the argument that $Sn^{4+}$ does not substitute for $W^{6+}$. Thus the notation for this centre is given as $W^{5+}$–$Sn_{Zn}^{4+}$ and a model to represent it is shown in figure 3(a). For comparison, models of the $V_O^{\cdot}$(B) and $W^{5+}$–H centres are depicted in figure 3(b).

From our results we cannot determine for certain whether the charge compensation of the $Sn_{Zn}^{4+}$ ion in the $ZnWO_4$ lattice is nonlocal or local. Should the former be so, the observed $C_1$ symmetry supplies additional evidence for the argument that the spin is localized mainly at the W. The reasoning is that if the spin were instead mainly located at Sn in a Zn site and nonlocally charge compensated, the defect would be expected to have $C_2$ symmetry and it

**Table 2.** Best-fit spin-Hamiltonian parameters of the $W^{5+}$–$Sn^{4+}_{Zn}$ centre are presented for comparison with the principal $g$ values and eigenvectors of the $V^{\cdot}_{O}$(B), $W^{5+}$–H and $Mo^{5+}$–H centres in $ZnWO_4$ single crystals. The HF tensors are for $W_1$ or Mo ($W_1$ site); the SHF tensors are for $W_2$ or Sn (Zn site); only the $\tilde{\mathbf{A}}$ tensors for isotopes $^{183}$W, $^{95}$Mo and $^{119}$Sn are given. Direction cosines of the dimensionless eigenvectors are defined with respect to the crystallographic axes [100], [010] and [001], respectively. Estimated uncertainties for eigenvector components of the $\tilde{\mathbf{g}}$, $\tilde{\mathbf{A}}_{W1}$ and $\tilde{\mathbf{A}}_{Sn}$ tensors for the $W^{5+}$–$Sn^{4+}_{Zn}$ centre are ±0.002, ±0.003 and ±0.003, respectively.

| | $\tilde{\mathbf{g}}$ | | | $\tilde{\mathbf{A}}_{W\ or\ Mo}$(HF) × $10^{-4}$ cm$^{-1}$ | | | $\tilde{\mathbf{A}}_{W\ or\ Sn}$(SHF) × $10^{-4}$ cm$^{-1}$ | | | |
|---|---|---|---|---|---|---|---|---|---|---|
| Centre | $g_{xx}$ | $g_{yy}$ | $g_{zz}$ | $A_{xx}$ | $A_{yy}$ | $A_{zz}$ | $A_{xx}$ | $A_{yy}$ | $A_{zz}$ | Refs |
| $W^{5+}$–H | 1.4911 | 1.3718 | 1.1513 | 58.5 | 61.3 | 148.7 | | | | |
| | 0.163 | −0.282 | 0.946 | 0.52 | −0.18 | 0.84 | | | | [16] |
| | 0.767 | −0.567 | −0.301 | 0.81 | −0.20 | −0.54 | | | | |
| | 0.621 | 0.774 | 0.124 | 0.26 | 0.96 | 0.04 | | | | |
| $Mo^{5+}$–H | 1.9021 | 1.8250 | 1.7021 | 28.2 | 32.0 | 79.8 | 22.2 | 26.0 | 30.0 | |
| | 0.096 | −0.178 | 0.979 | 0.575 | −0.226 | 0.786 | 0.516 | −0.850 | 0.116 | [17] |
| | 0.778 | −0.601 | −0.185 | 0.757 | −0.217 | −0.616 | 0.750 | 0.386 | −0.536 | |
| | 0.621 | 0.779 | 0.081 | 0.310 | 0.950 | 0.046 | 0.413 | 0.359 | 0.837 | |
| $W^{5+}$–$Sn^{4+}_{Zn}$ | 1.4675 ± 0.0002 | 1.6323 ± 0.0002 | 1.3821 ± 0.0002 | 73.1 ± 0.5 | 52.3 ± 0.5 | 126 ± 0.5 | 443.6 ± 0.5 | 448.5 ± 0.5 | 463.7 ± 0.5 | |
| | −0.014 | −0.162 | 0.987 | 0.478 | −0.283 | 0.831 | −0.120 | −0.383 | 0.916 | this |
| | 0.753 | −0.651 | −0.096 | 0.738 | −0.383 | −0.555 | 0.987 | −0.144 | 0.069 | work |
| | 0.658 | 0.742 | 0.131 | 0.476 | 0.879 | 0.026 | 0.106 | 0.912 | 0.396 | |
| $V^{\cdot}_{O}$(B) | 1.5409 | 1.5711 | 1.8185 | 36.9 | 68.2 | 96.4 | 21.6 | 23.0 | 28.0 | |
| | 0.236 | −0.105 | 0.966 | −0.333 | 0.367 | −0.869 | 0.675 | −0.736 | 0.043 | [15] |
| | 0.825 | −0.504 | −0.257 | 0.612 | −0.617 | −0.495 | 0.707 | 0.629 | −0.323 | |
| | 0.513 | 0.858 | −0.032 | 0.717 | 0.697 | 0.019 | 0.211 | 0.249 | 0.945 | |

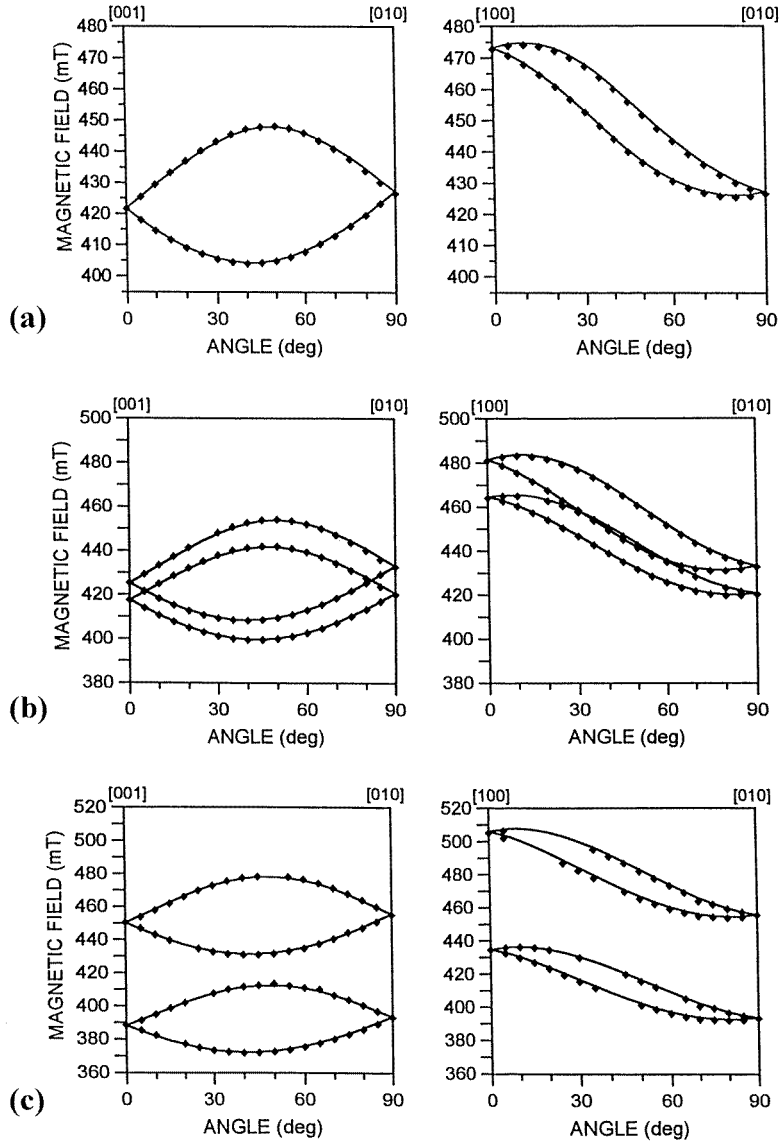


**Figure 2.** ESR angular variations in the (100) and (001) planes for the $W^{5+}$–$Sn^{4+}_{Zn}$ centre in a $ZnWO_4$ single crystal (the lines of both geometrical sites are presented). Symbols represent experimental data and the solid curves are computer-simulated angular variations calculated with the optimized spin-Hamiltonian parameters. Observations were made at ∼23 K and ∼9.2 GHz. (a) Variation of the central ESR lines (with no HF or SHF splitting). (b) Variation of the $^{183}W_1$ HF lines. (c) Variation of the $^{119}Sn$ SHF lines.

would have two equivalent W ions nearby. But this is not observed; instead, the symmetry is $C_1$. In fact the original $C_2$ symmetry of the W ion is reduced to $C_1$ because of the nearby Sn impurity. It should be mentioned that if $Sn^{4+}_{Zn}$ were nonlocally charge compensated, it would form a strong electron trap because of its net positive charge relative to the lattice; instead, however, the unpaired electron is mainly on the W. If one supposes a local charge compensator for the Sn (e.g., a Zn vacancy), the symmetry should also be $C_1$. Therefore, we cannot be

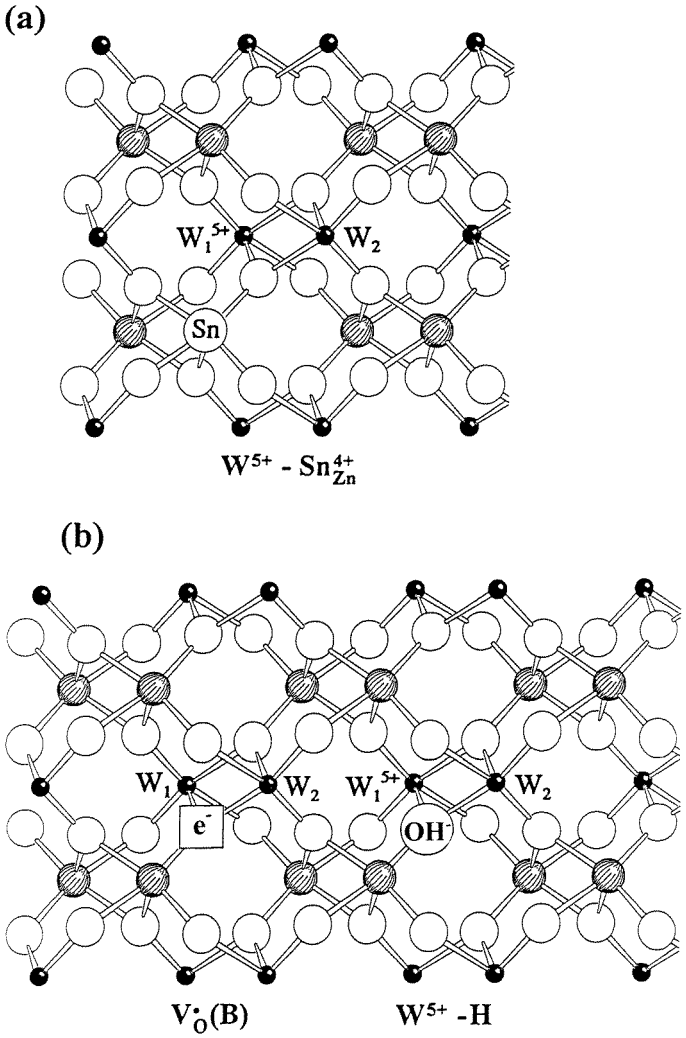


**Figure 3.** (a) Projection of the model of the $W^{5+}$–$Sn^{4+}_{Zn}$ centre in $ZnWO_4$ in the (001) plane, where the Sn is substituting for Zn. (b) For comparison, previously reported models of the $V_O^{\cdot}$(B) and $W^{5+}$–H centres are shown (on the same figure for convenience only). Filled, striped and open circles represent $W^{6+}$, $Zn^{2+}$ and $O^{2-}$ ions, respectively. The crystal models were prepared employing the SCHAKAL 92/V256 program (Kristallographisches Institut Freiburg).

certain whether the $C_1$ symmetry results primarily from the Sn ion near the W or from a local charge-compensating defect.

Although precise concentration measurements were not made, a rough estimate of the upper limit of the Sn defect concentration can be given. The Fe concentration in undoped $ZnWO_4$ was determined by atomic absorption spectroscopy to be 6.8 $\mu$mol mol$^{-1}$ [19]. A fraction of the Fe impurity is present in the crystal as $Fe^{3+}$ which can be measured easily by ESR. The relative concentration of the $W^{5+}$–$Sn^{4+}_{Zn}$ centre was always smaller by at least an order of magnitude than that of $Fe^{3+}$. Thus its concentration was smaller than 1 $\mu$mol mol$^{-1}$. Since by illumination at 77 K the concentration of the new defect saturated, it is believed that all or most of the available Sn impurity was transformed into this paramagnetic centre. If this

assumption is valid, then the total Sn concentration should also be less than 1 $\mu$mol mol$^{-1}$. All of the prepared crystals have shown the spectrum of the $W^{5+}$–$Sn^{4+}_{Zn}$ centre, which is the first evidence to our knowledge for the Sn impurity in $ZnWO_4$ crystals.

## 4. Summary

In undoped $ZnWO_4$ single crystals grown from different source materials a new paramagnetic impurity-related electron-type centre was produced by UV (365 nm) illumination at 77 K. The illumination liberates electrons from $Fe^{2+}$ impurity ions which are captured forming a new centre that has been characterized by ESR spectroscopy. Based on interpretations of HF and SHF interactions and spin-Hamiltonian parameters this defect is attributed to a $W^{5+}$ ion perturbed by a nearby Sn impurity. The Sn ion is shown to substitute for $Zn^{2+}$ in a 4+ charge state and the defect is denoted as the $W^{5+}$–$Sn^{4+}_{Zn}$ centre. Its concentration in the crystals studied is estimated to be below 1 $\mu$mol mol$^{-1}$.

## Acknowledgments

We are grateful to Dr V Grachev for providing his program 'VisualEPR' and Ms Á Péter, Ms Zs Tóth and Mr Gy Matók for growing and processing the crystals. This research was supported by the US National Science Foundation (grant No INT-9222297), the University of Connecticut Research Foundation and the National Science Research Foundation OTKA, Hungary (grant No T22859).

## References

[1] Oi T, Takagi K and Fukazawa T 1980 *Appl. Phys. Lett.* **36** 278
[2] Grabmaier B C 1984 *IEEE Trans. Nucl. Sci.* **31** 372
[3] Grassmann H, Moser H-G and Lorenz E 1985 *J. Lumin.* **33** 109
[4] Yamaga M, Marshall A, O'Donnell K P and Henderson B 1990 *J. Lumin.* **47** 65
[5] Földvári I, Capelletti R, Péter Á and Schmidt F 1987 *Solid State Commun.* **63** 787
[6] Watterich A, Wöhlecke M, Müller H, Raksányi K, Breitkopf A and Zelei B 1992 *J. Phys. Chem. Solids* **53** 889
[7] Földvári I, Capelletti R, Péter Á, Cravero I and Watterich A 1986 *Solid State Commun.* **59** 855
[8] Galkin A A, Neilo G N and Tsintsadze G A 1967 *Fiz. Tverd. Tela* **9** 359 (Engl. Transl. *Sov. Phys.–Solid State* **9** 275)
[9] Sroubek Z and Zdansky K 1966 *J. Chem. Phys.* **44** 3078
[10] Bates C A, Oglesby M J and Standley K J 1972 *J. Phys. C: Solid State Phys.* **5** 2949
[11] Watterich A, Edwards G J, Gilliam O R, Kappers L A, Madacsi D P, Raksányi K and Voszka R 1991 *J. Phys. Chem. Solids* **52** 449
[12] Nilsen W G and Kurtz S K 1964 *Phys. Rev.* **136** A262
[13] Kurtz S K and Nilsen W G 1962 *Phys. Rev.* **128** 1586
[14] Földvári I, Kappers L A, Gilliam O R, Hamilton D S, Lyu Li-Ji, Cravero I and Schmidt F 1990 *J. Phys. Chem. Solids* **51** 953
[15] Watterich A, Edwards G J, Gilliam O R, Kappers L A, Corradi G, Péter Á and Vajna B 1994 *J. Phys. Chem. Solids* **55** 881
[16] Watterich A, Gilliam O R, Kappers L A and Raksányi K 1996 *Solid State Commun.* **97** 477
[17] Watterich A, Hofstaetter A, Wuerz R, Scharmann A and Gilliam O R 1998 *J. Phys.: Condens. Matter* **10** 205
[18] Schmidt F and Voszka R 1981 *Cryst. Res. Technol.* **16** K127
[19] Bencs L F, Raksányi K, Szakács O, Kovács L, Watterich A and Péter Á 1997 *J. Cryst. Growth* **181** 455
[20] Wyckoff R W G 1965 *Crystal Structures* 2nd edn, vol 3 (New York: Interscience) pp 41–3
[21] Schofield P F, Knight K S and Cressey G 1996 *J. Mater. Sci.* **31** 2873
[22] Lide D R (ed) 1998 *Handbook of Chemistry and Physics* 79th edn (New York: Chemical Rubber Company)
[23] Solntsev V P and Khranenko G G 1989 *Fiz. Tverd. Tela* **31** 292 (Engl. Transl. *Sov. Phys.–Solid State* **31** 1823)